JOURNAL OF CATALYSIS **169,** 347–358 (1997)
ARTICLE NO. CA971712

Characterization of a Mo/ZSM-5 Catalyst for the Conversion of Methane to Benzene

Dingjun Wang, Jack H. Lunsford, and Michael P. Rosynek[1]

Department of Chemistry, Texas A&M University, College Station, Texas 77843

Received January 10, 1997; revised March 24, 1997; accepted April 2, 1997

The dehydroaromatization of methane to benzene has been investigated over a 2 wt% Mo/ZSM-5 catalyst in the absence of an added oxidant. The reaction is characterized by an induction period, prior to the initiation of benzene production, during which Mo_2C is formed and coke deposition occurs. The formation of the carbide was confirmed by X-ray photoelectron spectroscopy (XPS) measurements. Pretreatment of the catalyst in a CH_4/H_2 gas mixture at 700°C reduces Mo^{6+} ions in the calcined catalyst into Mo_2C and almost eliminates the induction period, confirming that Mo_2C is the active species in the activation of methane. Under typical CH_4 reaction conditions at 700°C, 60–80% of the original Mo^{6+} ions are reduced to form Mo_2C, with the remaining Mo occurring primarily as Mo^{4+} and traces of Mo^{5+} ions. These nonreducible Mo ions are most likely within the channels of the zeolite. XPS, ion-scattering spectroscopy, and FT-IR measurements indicate that Mo species in a Mo/ZSM-5 sample dried at 130°C are present as small (30 to 50 Å) crystallites of the original ammonium heptamolybdate impregnated salt on the external surface of the zeolite. After calcination at higher temperatures (500–700°C), Mo becomes more highly dispersed, but not uniformly distributed, on the external surface of the zeolite. During preparation and/or pretreatment of the catalyst, a portion of the Mo ions diffuses into the channels of the zeolite. The amount of Mo ions within the channels depends on the temperature, time, and atmosphere of calcination. The roles of Mo_2C, partially reduced Mo ions, and the origin of the induction period are discussed on the basis of kinetic results and physical/chemical characterization measurements of the catalyst.

INTRODUCTION

Direct conversion of methane to higher hydrocarbons, particularly to aromatics such as benzene, toluene, and naphthalene, in the absence of gas-phase oxygen has received considerable recent attention. Although the formation of aromatic products from CH_4 in the absence of O_2 is not thermodynamically favorable at low temperatures (<500°C), the equilibrium CH_4 conversion at 700°C is ~12%. At this temperature, benzene and naphthalene, in approximately equimolar amounts, are the thermodynamically preferred products. The thermodynamic equilibrium composition of the C–H system (excluding graphite) at 1 atm pressure is shown in Fig. 1 for the temperature range 500–1200°C.

Bragin *et al.* (1) have carried out the aromatization reaction of methane to benzene in a pulse reactor over a $Pt–CrO_3/HZSM$-5 catalyst at 750°C. A methane conversion of 18% with 80% selectivity to benzene was achieved. Belgued *et al.* (2) found that exposure of a supported Pt catalyst to pure methane, followed by hydrogenation, can result in the formation of aliphatic hydrocarbons containing up to six carbon atoms. Formation of C_2 to C_6 alkanes from methane in a two-step route was also achieved on Group VIII transition metal catalysts (3). None of these previously reported processes, however, was carried out in a continuous-flow reactor.

Several recent studies of methane conversion to aromatics have been carried out over MoO_3/ZSM-5 catalysts in flow reactors. Wang *et al.* (4) reported that a methane conversion of 7% could be achieved at a benzene selectivity of 100%. Solymosi and co-workers (5–8) observed a benzene selectivity of ~65% at a methane conversion of 5.7%. In our previous investigations (9, 10), we observed that, following an initial induction period, a benzene selectivity of ~70% at a methane conversion of 8% could be sustained for more than 16 h. Although a similar catalytic performance has been reported by several groups for CH_4 conversion over Mo/ZSM-5, differing active sites, reaction mechanisms, and reaction intermediates have been proposed (5, 10–13) by the various investigators.

One group (11, 14–16), for example, has suggested that MoO_3 may be involved as the catalytically active center, and that dimerization of a $CH_2{=}MoO_3$ species occurs to produce ethylene as the reaction intermediate. They assumed that methane may be heterolytically split to CH_3^+ and H^- over the acid sites in the channels of the ZSM-5 zeolite (11), and that molybdenum species in a high oxidation state promote such heterolytic dissociation of the C–H bond. Based on XPS results, they proposed that methane activation may be associated with Mo^{6+}, Mo^{5+}, and Mo^{4+} ions (15). In this reaction scheme, however, the role of

[1] To whom correspondence should be addressed.

0021-9517/97 $25.00

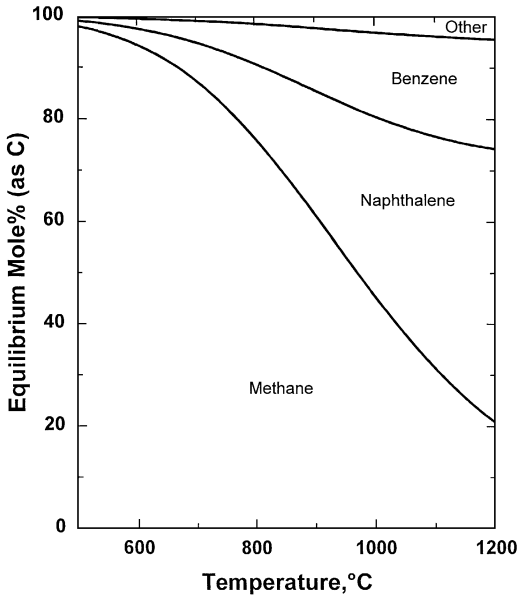

FIG. 1. Effect of temperature on the thermodynamic equilibrium composition of the C–H system (excluding graphite) at 1 atm pressure.

acid sites in the activation of methane, as suggested earlier, was not addressed. Chen and co-workers (12) carried out X-ray photoelectron spectroscopy (XPS), electron spin resonance, and temperature-programmed reduction measurements of fresh and used Mo/ZSM-5 catalysts and concluded that methane was activated to form CH_3· radicals via a synergistic action between MoO_x and Brønsted acidic sites, and that ethane, rather than ethylene, was produced as the primary product. These authors propose that the active oxygen species is removed during the reaction by the reduction of molybdenum ions by methane. Solymosi and co-workers (5) investigated the dehydrogenation of methane on various supported MoO_3 catalysts, including MoO_3/SiO_2 and MoO_3/ZSM-5, and proposed that partially reduced molybdenum ions, probably Mo^{4+}, are responsible for the activation of methane, and particularly for the formation of benzene.

By contrast, in our previous studies (9, 10) we demonstrated that exposure of a calcined Mo/ZSM-5 catalyst to CH_4 at 700°C causes reduction of molybdenum ions to the carbide, Mo_2C, which was identified by XPS. Disappearance of Mo^{6+} from the original MoO_3 and formation of Mo_2C were virtually complete after exposure of the calcined catalyst to CH_4 for 2 h, which corresponds to the time of the initial activation period. It was suggested that Mo_2C may be the active species responsible for the initial activation of methane. This proposal was supported by the observations that unsupported Mo_2C can also activate methane, and that the addition of CO_2 to the reactant stream reoxidizes Mo_2C to Mo^{6+}, Mo^{5+}, and Mo^{4+} ions, causing a complete loss of activity for the formation of benzene. In their most recent studies, Solymosi and co-workers (6–8) have also concluded that MoC_2 is involved in the initial activation of CH_4 over Mo/ZSM-5. Discrepancies among various groups in identifying the active molybdenum species for CH_4 activation may result from the different sample treatments that have been employed prior to obtaining XPS spectra, since Mo_2C is readily reoxidized when exposed to air, even for a short time. Another difficulty in confirming the formation of Mo_2C by XPS measurements is that the carbidic C1*s* signal overlaps with that of abundant other forms of surface carbon, particularly coke, that are formed under typical reaction conditions (10).

An additional area of disagreement concerns the distribution of Mo in the ZSM-5 zeolite. No conclusive evidence has been reported in previous investigations regarding the location of Mo in the zeolite, although most researchers agree that molybdenum ions are highly dispersed and are distributed through the zeolite channels (4, 6, 9–12, 14–18). Based on X-ray diffraction (XRD), BET, and NH_3 adsorption/desorption results, Guo and co-workers (11, 14, 16) and Lin and co-workers (12) have suggested that Mo may be in a highly dispersed state in their 2% Mo/ZSM-5 catalysts. However, when the Mo loading was in the range 6 to 10 wt%, the presence of crystalline MoO_3 was confirmed by XRD and FT-IR measurements. At this level of Mo loading, the BET surface area (11, 12, 16), micropore volume (11, 12), ZSM-5 crystallinity (11), NH_3 uptake/desorption (12, 14, 16), and activity of the catalyst for the conversion of methane (11, 12) all decreased significantly from their values at 2 wt% Mo loading. These results were interpreted as evidence that Mo was located within the channels of the ZSM-5 (11, 12, 16). However, it is difficult to determine whether the decreases in surface area and NH_3 uptake result from extensive blockage of the channel entrances or are due to migration of Mo within the channels. The amount of Mo needed for monolayer coverage on the external surface of ZSM-5, assuming a crystallite size of 0.3 μm and uniform Mo distribution, for example, is only about 0.6 wt%. Therefore, it is very likely that the formation of multilayers of Mo oxides that occur at high Mo loadings may result in extensive blockage of the channel entrances. When the Mo loading is high and the sample is calcined at high temperature, e.g., at 700°C for several hours, Mo may diffuse into the zeolite channels. However, because the activity for methane conversion decreases significantly at high Mo loadings (11, 12), no conclusion can be made regarding the distribution of the active Mo species in the ZSM-5 zeolite.

Based on characterizations by XRD, acidity and catalytic activity for Brønsted acid-catalyzed reactions, Valyon and Meszaros-Kis (19) suggested that Mo in a conventionally prepared Mo-impregnated HZSM-5 sample is located primarily on the external zeolite surface, but that Mo could be homogeneously distributed inside the channels of the

zeolite by contacting HZSM-5 with $Mo(x\text{-}C_3H_5)_4$ in pentane. In a study of a Mo/ZSM-5 (Si/Al = 400) catalyst used for hydrodesulfurization reactions, Fierro and co-workers (20, 21) concluded that most of the Mo exists as MoO_3 on the external zeolite surface.

In the present investigation, we have addressed in greater detail than previously the formation of Mo_2C and the role of the carbidic species in the conversion of methane to aromatic products, based on results of kinetic and XPS measurements of a Mo/ZSM-5 catalyst under well-controlled pretreatment conditions. The role of the carbide in activating CH_4 was explored by intentionally preparing Mo_2C on the ZSM-5 support and comparing its catalytic behavior to that of a catalyst originating as MoO_3/ZSM-5. In addition, XPS, ISS, and FT-IR techniques were employed to provide greater insight into the distribution of molybdenum in the ZSM-5 zeolite. Particular emphasis was placed on elucidating the differing behaviors of the Mo located on the external surface of the zeolite support and that located within the zeolitic channels.

EXPERIMENTAL

Catalyst Preparation

The catalyst was prepared by making a slurry of 10 g of H-ZSM-5 (Conteka B.V. 5020, Si/Al = 25) in 20 ml of an aqueous solution containing the desired amount of ammonium heptamolybdate $[(NH_4)_6Mo_7O_{24}]$ at 85°C for 16 h, followed by drying for 4 h at 120°C and then calcining for 4 h at 500°C in air. The calcined samples were crushed and sieved to 20/45 mesh granules. Since all of the Mo-containing solution was deposited onto the H-ZSM-5 support during drying, the Mo content in the final catalyst was assumed to be the same as the total Mo content of the solution, and was not separately analyzed. All experiments were performed using 2 wt% Mo/ZSM-5 samples.

Reactor System

Reactions were carried out in a flow system, using reactors constructed from alumina tubes (Coors, AD-998, 99.8% Al_2O_3) having an i.d. of 6.4 mm and using 1.0 g of catalyst, unless otherwise specified. To minimize the contribution from gas-phase reactions, quartz chips were used to fill the space above and below the catalyst beds in the flow reactors. A thermocouple in a smaller alumina tube was attached to the outside wall of each of the reactors for temperature measurement and control.

Reactant and pretreatment gases, which included 10% N_2/CH_4, O_2, He, and H_2, were all of UHP grade from Matheson and were used without further purification. Gas flows were regulated by mass flow controllers. In a typical experiment, the catalyst was first heated in the flow reactor in a stream of He at 700°C for 1 h. Before introducing the 10% N_2/CH_4 reactant gas mixture into the reactor, the catalyst was further heated in an O_2 flow at 700°C for 0.5 h and then flushed in He for 1 h at the same temperature. The 10% N_2 in the CH_4 reactant was used as an inert internal standard to enable accurate determinations of CH_4 conversions (typically <10%) and to allow quantitative evaluation of coke formation during the reaction from carbon mass balances. The reaction mixtures were analyzed by on-line gas chromatography using a column containing 5% Bentone 34 on Chromosorb W-AW for separation of aromatic products and a HayeSep D column for separation of CO_x and other hydrocarbons. All studies were carried out at atmospheric pressure, without diluting the reagents with additional inert gas.

Catalyst Characterization

XPS and ion-scattering spectroscopy (ISS) spectra, which were used to determine the abundance and chemical state of surface components of the catalysts, were acquired using a Perkin–Elmer (PHI) Model 5500 spectrometer. All spectra were obtained using samples prepared in the form of pressed wafers and treated in one of two ways: (i) "fresh" samples were prepared by treatment in a separate quartz reactor system in a stream of O_2 at various desired temperatures; and (ii) "used" samples were prepared by treating the fresh catalysts in 10–20% CH_4/H_2 and/or pure CH_4 at 700°C, duplicating the conditions employed in the catalytic reaction experiments. The quartz reactor system used for these treatments contained an O-ring-sealed port that allowed *in situ* transfer of the ceramic holder containing the treated sample into a stainless-steel vacuum transport vessel (PHI Model 609217). The removable vessel was then transferred to a similar port on the inlet system of the XPS spectrometer, which was subsequently evacuated, allowing the sample to be introduced into the UHV analysis chamber of the instrument using magnetically coupled transfer rods without exposure to the air. A typical XPS data acquisition employed a pass energy of 29.35 eV, a step increment of 0.125 eV, and a Mg anode power of 400 W. All binding energies were referenced to the zeolitic Al2*p* line at 74.5 eV. Near-surface compositions were calculated from peak areas using appropriate sensitivity factors. ISS spectra were obtained using $^3He^+$ ions at a scattering angle of 134.5° and ~1 kV accelerating potential. To avoid any charging effects of the insulating catalysts, which would distort the ion energy spectra, the specimens were flooded with thermal electrons during ISS data acquisition.

Infrared spectra were obtained using a Perkin–Elmer Model 2000 FT-IR spectrometer. Self-supporting wafers having an optical density of 10–15 mg/cm^2 were pressed from the powdered catalysts. The wafers were mounted on a fused quartz bracket that was placed in an IR cell equipped with KBr windows and a heated region into which the wafer could be moved for thermal treatment. The catalyst samples used in the IR study were subjected to the same

pretreatments as those used in the XPS and ISS experiments. Following the desired *in situ* pretreatment, spectra were recorded at a resolution of 4 cm^{-1} with the sample at room temperature. Corrections for variation in sample wafer thickness were made for all the spectra.

RESULTS AND DISCUSSION

Catalytic Results

In our previous studies (9, 10), it was shown that, following an initial induction period, during which the CH_4 reactant reduces the original Mo^{6+} ions in the zeolite to Mo_2C and deposition of coke occurs, a benzene selectivity of about 70% at a CH_4 conversion of 8% could be sustained for 16 h over a 2 wt% Mo/ZSM-5 catalyst at 700°C. Because metallic Mo^0 and the Mo in Mo_2C cannot be readily distinguished in XPS spectra due to the similarity in Mo3*d* binding energies of these two species (22–24), it is necessary to use the C1*s* peak of Mo_2C to determine the Mo/C ratio and confirm the formation of Mo_2C during the reaction. Under normal reaction conditions, the presence of a large amount of coke on the catalyst surface prevents unambiguous identification of Mo_2C and the role of Mo_2C in the reaction. Therefore, to understand the origin of the induction period and confirm formation of Mo_2C, it was necessary to form Mo_2C in the zeolite without significant concomitant deposition of coke. Based on the studies of Boudart and co-workers on the formation of molybdenum carbides from MoO_3 (25, 26), it is possible to form Mo_2C without significant formation of graphitic or coke-like carbon by treating MoO_3 in a 20% CH_4/H_2 flow at 670°C.

Figure 2 shows methane conversions and benzene selectivities for the reaction of methane in the absence of gas-phase oxygen at 700°C and at a space velocity of 800 h^{-1} over a 2 wt% Mo/ZSM-5 catalyst pretreated under different conditions. The solid data points depict typical results obtained over a catalyst sample that had been pretreated in O_2 for 0.5 h and then in He for 0.5 h at 700°C prior to initiating the 10% N_2/CH_4 reactant flow. The open data points display the results obtained over a catalyst which had been treated at 700°C in a 200 ml/min flow of 20% CH_4/H_2 for 12 h, followed by a flow of 10% CH_4/H_2 at the same temperature for 4 h. The conversion of CH_4 to benzene was confirmed to be a catalytic process, rather than a merely stoichiometric reduction of Mo ions, since the ratio of CH_4 molecules reacted to total Mo atom content in the catalyst was >100 over a 10-h period on stream. Under steady-state conditions at 700°C, the rate of CH_4 conversion over the 2 wt% Mo/ZSM-5 catalyst was ca. 1 μmol/g/s, equivalent to 0.0048 mol/mol Mo/s or 17 CH_4/Mo/h.

Following an initial activation period during the first 2 h of reaction, a benzene selectivity of 60 to 65% at a CH_4 conversion of 4 to 8% was achieved over the sample calcined in O_2. (Both the CH_4 conversions and the benzene selectivities shown in Fig. 2 are slightly lower than those we reported previously (9, 10), primarily due to improved accuracy in determining CH_4 conversion levels resulting from the use of a 10% N_2 internal standard instead of the 1% N_2 employed in our earlier study.) During this induction period, particularly during the first 10 to 20 min, virtually no hydrocarbon products were formed, and the principal gas-phase products resulting from CH_4 conversion were H_2, CO, CO_2, and H_2O (see Fig. 3a). The total selectivity to gas-phase products was also low because significant amounts of coke and Mo_2C were formed from CH_4 during this initial period, accounting for the remainder of the selectivity not shown in Figs. 2 and 3. Following the initial induction period, however, the amount of coke that continued to form from CH_4 reactant corresponded to ~15% of the CH_4 converted. The selectivity to naphthalene attained a maximum of ~16% immediately following the initial activation period, but then declined rapidly with increasing time on stream. Presumably the gradual accumulation of coke in the zeolite channels decreased their effective diameter, thus increasingly inhibiting the formation (or escape) of the thermodynamically favored, but bulky, naphthalene molecules (10). Thus, after a sufficiently long period of reaction, benzene and a small amount of toluene were selectively produced as the *kinetically* favored aromatic products. The selectivity to C_2–C_3 hydrocarbons (which were mainly ethylene), although always small compared to that of benzene, increased continuously with increasing reaction time, as coke deposition gradually deactivated the acidic sites in the zeolite where the ethylene primary product undergoes secondary reactions (10). In all cases, the original activity and selectivity behaviors of the catalyst, including the initial induction

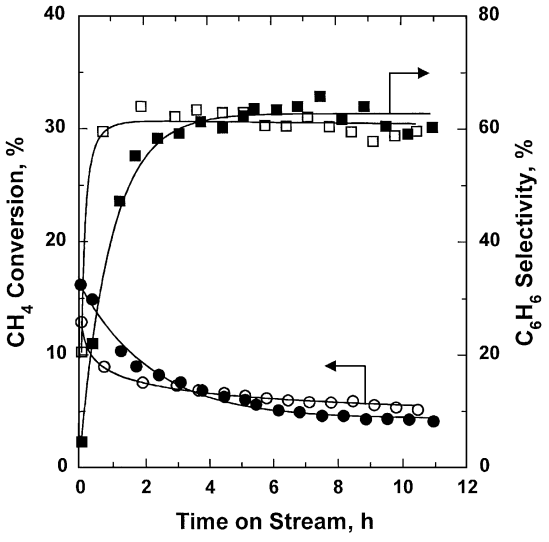

FIG. 2. Methane conversion and benzene selectivity for CH_4 reaction over 2 wt% Mo/ZSM-5 at 700°C, 1 atm, and GHSV = 800 h^{-1}. ●, ■, pretreated in O_2 at 700°C; ○, □, pretreated in 20% CH_4/H_2 and then in 10% CH_4/H_2 at 700°C, following treatment in O_2 at 700°C for 0.5 h.

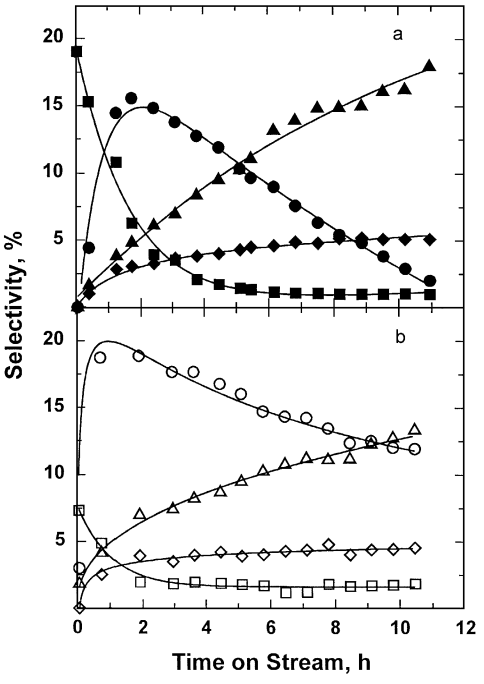

FIG. 3. Selectivity results for CH_4 reaction over 2 wt% Mo/ZSM-5 at 700°C, 1 atm, and GHSV = 800 h^{-1}. ●, ○, naphthalene; ◆, ◇, $C_2 + C_3$; ▲, △, toluene; ■, □, CO. (a) Pretreated in O_2 at 700°C for 0.5 h; (b) pretreated in 20% CH_4/H_2 for 12 h and then in 10% CH_4/H_2 for 4 h at 700°C, following treatment in O_2 at 700°C for 0.5 h.

period, could be completely restored by retreating the used catalyst in O_2 at 700°C.

By contrast, the induction period was largely, although not completely, eliminated when the catalyst was pretreated in the CH_4/H_2 gas mixture (open data points in Figs. 2 and 3). In this case, significant amounts of hydrocarbons, mainly benzene and naphthalene, were produced even during the first few minutes of reaction. Only very small amounts of CO_2 and H_2O were detected, and the amount of CO formed (Fig. 3b) was much smaller than that observed over the calcined sample that had not been prereduced (Fig. 3a). In addition, the selectivity to naphthalene not only attained a larger maximum value of ~20% following the initial activation period, but then also declined much more slowly with increasing time on stream, in comparison to that observed over the unreduced catalyst (Fig. 3a). Presumably, a decrease in the concentration of acidic sites after the pretreatment in CH_4/H_2 may suppress the deposition of coke in the zeolite channels so that the formation of naphthalene becomes less inhibited. Although the rate of deactivation of the prereduced catalyst also appears to be somewhat slower than that of the calcined sample, the overall catalytic performances, following the initial induction period, are very similar for both samples. These results, together with the XPS data to be described below, indicate that formation of Mo_2C during the CH_4/H_2 pretreatment is virtually complete, and suggest that the induction period observed for the calcined catalyst is due to the formation of Mo_2C, which is the active species for the activation of methane.

The fact that the extended pretreatment at 700°C in CH_4/H_2 did not completely eliminate the induction period observed with the calcined catalyst indicates that the reduction of Mo, although necessary, is not solely responsible for the observed induction period (9, 10). Additional modification of the Mo-containing sites, possibly involving partial deactivation by coke deposition on Mo_2C, may be required to create sites that selectively convert CH_4 to higher hydrocarbon products. The deposition of carbonaceous materials on Mo_2C during the induction period is evidenced by the decreased intensity of the Mo3*d* XPS bands after a catalyst had been exposed to CH_4 reactant for 2 h (see below). It is possible that the fresh carbidic surface, formed by treating Mo/ZSM-5 in a CH_4/H_2 gas mixture, is efficient for methane activation, but may be too reactive for the formation and/or desorption of the ethylene primary product.

The beneficial effects of carbonaceous deposits have been observed previously for various reactions over metal carbide catalysts and have been attributed to a site-blocking effect (27–29) and/or electronic modification of the active surface as a result of the metal–carbon bond formation (29, 30). Wang and Tysoe (29) carried out an investigation of ethylene hydrogenation over metallic molybdenum and found that the reaction was facilitated both by the formation of molybdenum carbide and by the deposit of carbonaceous material. They suggested that part of the role of the carbonaceous deposit was to block extremely active sites to prevent further hydrocarbon decomposition. In a study of selective activation of C–H and C=C bonds on metal carbides, Chen (30) observed that the interaction between 1,3-butadiene and a vanadium carbide surface is sufficiently strong that decomposition of 1,3-butadiene occurred on the carbide surface with a C/V ratio of 1.

The small remaining induction period after prereduction in CH_4/H_2 might also be attributed to incomplete reduction of molybdenum oxides to Mo_2C (see below). Indeed, XPS and ISS experiments confirm that the surface oxygen concentration on an unsupported Mo_2C sample prepared from MoO_3 can be as high as 1 to 3%, even after it had been reduced in a CH_4/H_2 gas mixture at 700°C for 16 h. However, in a separate experiment, it was observed that when methane was replaced by an equivalent amount of ethylene as the reactant gas after the original reaction had reached steady state, another induction period for the formation of benzene occurred. This second induction period reflects the fact that ethylene decomposes on the carbidic surface more readily than does methane, and that further coke decomposition occurs from ethylene on the already coked Mo_2C surface. However, the formation of CO, indicative of MoO_x reduction, did not increase after methane reactant was replaced by ethylene. These results suggest, therefore, that

incomplete reduction of molybdenum oxides is not responsible for the "residual" induction period.

Chemical States of Mo in the Catalysts

Since metallic Mo^0 and the Mo in Mo_2C cannot be readily distinguished in XPS spectra due to the similarity in Mo3*d* binding energies of these two species (29–31), it is necessary to use the C1*s* band of Mo_2C to determine the Mo/C ratio of the carbide, if it is formed during the reaction. Figures 4 and 5 show XPS spectra of the 2% Mo/ZSM-5 catalyst in the C1*s* and Mo3*d* regions, respectively. An unsupported molybdenum carbide sample, prepared by treating MoO_3 in a CH_4/H_2 gas mixture at 700°C for 16 h, is included for a comparison. (The formation of bulk molybdenum carbide, in the form of β-Mo_2C, from pure MoO_3 as the sole product following this treatment was confirmed by separate powder XRD measurements.) The carbided zeolite sample was similarly prepared by treating the 2 wt% Mo/ZSM-5 catalyst in a 200 ml/min flow of 20% CH_4/H_2 for 12 h at 700°C, followed by 10% CH_4/H_2 at the same temperature for 4 h. Table 1 provides a comparison of the various C1*s* and Mo3*d* binding energies observed in the present study to those reported by previous investigators.

As shown in Fig. 4a, only a small amount of graphitic carbon (characterized by the C1*s* peak at 284.6 eV) remains on the surface of the catalyst after calcination in O_2 at 700°C for 0.5 h. Exposure of the sample to CH_4 at the same temperature for 2 h results in the formation of a large amount of coke, giving rise to the intense peak at 283.5 eV, which obscures the Mo_2C that is also formed. (The lower C1*s* binding energy of this carbonaceous material, compared to that of graphitic carbon, suggests that it may be a hydrogen-poor sp-type of "pregraphitic" carbon.) However, coke formation is largely suppressed when the catalyst is reduced in a CH_4/H_2 mixture (Fig. 4c and Table 2), allowing a shoulder to become evident at 282.7 eV, which is consistent with the formation of Mo_2C (Fig. 4d). This result clearly demonstrates that molybdenum carbide is formed during pretreatment in the CH_4/H_2 gas mixture. Since the driving force for the formation of carbide from the oxide precursor increases as the concentration of methane in the gas mixture increases (22), it is reasonable to expect that molybdenum carbide is also formed under typical reaction conditions, i.e., in the presence of pure CH_4 reactant.

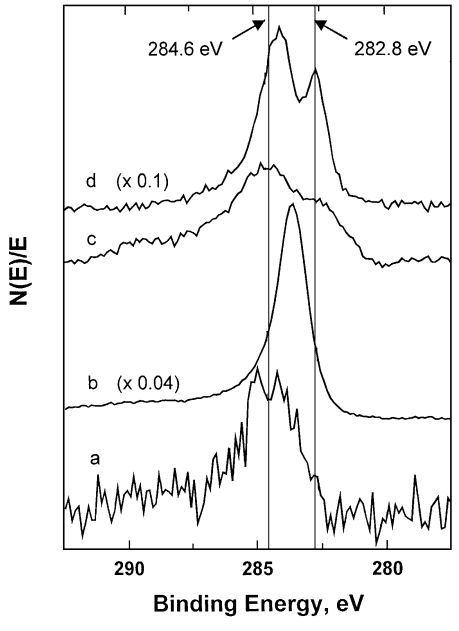

FIG. 4. XPS spectra of 2 wt% Mo/ZSM-5 and Mo_2C in C1*s* region. (a) Mo/ZSM-5 after calcination in O_2 at 700°C; (b) after subsequent exposure to CH_4 at 700°C for 2 h; (c) fresh sample pretreated at 700°C in 20% CH_4/H_2 for 12 h and then in 10% CH_4/H_2 for 4 h, following treatment in O_2 at 700°C, (d) unsupported Mo_2C, made by calcining MoO_3 at 700°C in flowing O_2 and then treating at 700°C in 20% CH_4/H_2 for 12 h and in 10% CH_4/H_2 for 4 h.

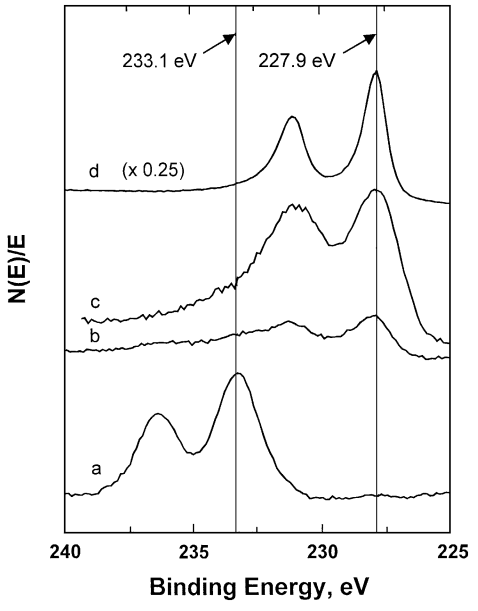

FIG. 5. XPS spectra of 2 wt% Mo/ZSM-5 and Mo_2C in Mo3*d* region. (a) Mo/ZSM-5 after calcination in O_2 at 700°C; (b) after subsequent exposure to CH_4 at 700°C for 2 h; (c) fresh sample pretreated at 700°C in 20% CH_4/H_2 for 12 h and then in 10% CH_4/H_2 for 4 h, following treatment in O_2 at 700°C; (d) unsupported Mo_2C, made by calcining MoO_3 at 700°C in flowing O_2 and then treating at 700°C in 20% CH_4/H_2 for 12 h and in 10% CH_4/H_2 for 4 h.

Formation of molybdenum carbide during the reaction of CH_4 is further supported by XPS spectra in the Mo3*d* region. As shown in Fig. 5, the molybdenum species present in the freshly calcined catalyst, based on the observed Mo3*d* binding energies, is mainly Mo^{6+} (10, 31, 36). After the sample was exposed to methane at 700°C for 2 h, which corresponds to the steady state achieved for the catalytic reaction (Fig. 2), the original Mo^{6+} ions were almost completely reduced. In addition, however, the overall intensity of all

TABLE 1

Summary of XPS Binding Energies (eV) Observed for Mo and C

Mo3$d_{5/2}$				C1*s*			
Mo (VI)	Mo (IV)	Mo (0)	Mo_2C	Graphitic	Coke	Carbidic	Ref.
233.0[a]	229.8[b]		227.8[c]			283.8[c]	8
232.7[d]			227.9[e]			283.8[e]	8
232.5	230.0	227.9	228.4	284.5		283.3	22
232.6	229.6		228.3				23
			227.8				24
232.6	229.1	227.8					31
232.8	229.6	227.9	228.6				32
						282.7	33
233.1	231.5	228.8					34
				284.2		282.9	35
233.1[d]			227.9[f]	284.6	283.5[f]	282.7[g]	This work

[a] Unsupported MoO_3.
[b] Unsupported MoO_2.
[c] Prepared from MoO_3 by treatment with H_2/CH_4 at 700°C.
[d] MoO_3/ZSM-5.
[e] Mo_2C/ZSM-5.
[f] After exposure to CH_4 for 2 h at 700°C.
[g] Prepared from MoO_3/ZSM-5 by treatment with H_2/CH_4 at 700°C.

of the Mo3*d* bands gradually decreased as the reduction time increased to 2 h (10). This decrease in intensity of the Mo3*d* bands can be ascribed to the deposition of carbonaceous material (i.e., coke) on the catalyst, as evidenced by the corresponding XPS spectra in the C1*s* region, shown in Fig. 4b. A similar reduction of Mo^{6+} occurred when the freshly calcined 2% Mo/ZSM-5 was treated in a flow of 20% CH_4/H_2 for 12 h, followed by 10% CH_4/H_2 at 700°C for 4 h. In this case, however, the intensity of the Mo3*d* bands remained essentially the same as before reduction (Fig. 5c), which is consistent with the fact that only a small amount of coke is formed during such a pretreatment (Fig. 4c and Table 2). The Mo3$d_{5/2}$ binding energy of 227.9 eV of the samples, pretreated either in the CH_4 or in the CH_4/H_2 gas mixture, is consistent with that of pure Mo_2C (Fig. 5d), as reported previously (10, 22–24).

The near-surface compositions of the catalyst, following different pretreatments, are summarized in Table 2. The relative amounts of the various carbon and molybdenum species were obtained by deconvolution of the C1*s* and Mo3*d* bands (Figs. 4 and 5), using the following assumptions: (i) Different full widths at half maximum (FWHM) were used for the same peak in the supported vs. the unsupported samples, due to different charging effects; however, the same FWHM was assumed for all peaks of the same sample. FWHM values of 1.1 and 2.3 eV were employed in the deconvolution of the C1*s* bands of the pure Mo_2C sample and the 2% Mo/ZSM-5 catalyst, respectively. For the Mo3*d* bands, FWHM values of 1.0 and 2.2 eV were used for the pure Mo_2C sample and the 2% Mo/ZSM-5 catalyst, respectively. (ii) Based on the results of the present study and those of previous investigators (8, 22, 23, 31, 32, 34), the Mo3$d_{5/2}$ and 3$d_{3/2}$ binding energies were assumed to be 233.1 and 236.3 eV for Mo^{6+}; 231.4 and 234.6 eV for Mo^{5+}; 229.3 and 232.5 eV for Mo^{4+}; and 227.9 and 231.1 eV for Mo_2C. The C1*s* binding energies were those shown in Table 1, viz., 284.6 eV for graphitic carbon, 283.5 eV for coke-like carbon, and 282.7 eV for carbidic carbon (8, 22, 33, 35).

Deconvolution of the Mo3*d* bands confirmed that ~90% of the molybdenum ions in the original oxidized catalyst (Fig. 5a) were Mo^{6+}, with the remaining 10% occurring as Mo^{5+}, probably resulting from photoreduction of the sample during X-ray irradiation in the spectrometer. After the sample was exposed to methane at 700°C for 2 h (Fig. 5b), 65% of the molybdenum species had been converted to Mo_2C. The remaining molybdenum was present as Mo^{4+} (20%) and Mo^{5+} (10%). Although a small amount of Mo^{6+} (<5%) may also have still been present after only 2 h of CH_4 reaction, it disappeared completely after 10 h of reaction time. Similar deconvolution results were obtained for the sample pretreated in the CH_4/H_2 gas mixture (Fig. 5c). The relative concentrations of Mo_2C, Mo^{4+}, and Mo^{5+} in this case were found to be 75, 20, and 5%, respectively. Based on the absolute near-surface concentrations of carbidic C and of Mo in the form of Mo_2C, the C/Mo ratio was determined to be 0.60, which is close to the stoichiometric value for Mo_2C. Using the same procedure, a C/Mo ratio of 0.59 was found for the unsupported Mo_2C sample.

These results clearly demonstrate that Mo_2C, and not metallic molybdenum, is formed under CH_4 reaction conditions at 700°C and, furthermore, that the carbide is most likely the active species for the activation of methane and formation of ethylene as the primary reaction intermediate (10). In fact, as discussed above, metallic Mo, if present,

TABLE 2

Near-Surface Compositions of Catalysts Determined by XPS Analysis[a]

					C(1*s*)		
Sample	Conditions	O1*s*	Si2*p*	Al2*p*	Graph +coke	Mo_2C	Mo3*d*
2 wt% Mo/ZSM-5	Calcined[b]	68.5	28.1	1.2	0.9	—	1.3
2 wt% Mo/ZSM-5	Used[c]	35.5	17.5	0.8	45.6[d]	—	0.6
2 wt% Mo/ZSM-5	Reduced[e]	66.7	29.6	1.2	0.9	0.5	1.1
MoO_3	Reduced[e]	—	—	—	42.6	18.9	37.9

[a] Atom% concentration.
[b] Sample was calcined at 700°C in flowing O_2 for 0.5 h.
[c] Sample was subsequently treated at 700°C in flowing CH_4 for 2 h.
[d] Total carbon concentration, including coke, graphitic carbon, and carbidic carbon.
[e] Samples were first calcined at 700°C in flowing O_2, and then treated at 700°C in 20% CH_4/H_2 flow for 12 h and in 10% CH_4/H_2 for 4 h.

would be catalytically inferior to carbidic Mo for the activation of C–H bonds and formation of ethylene. In addition, it has been observed in our previous study that addition of 80 Torr of CO_2 to the CH_4 feed, after having attained steady-state conditions, causes an immediate cessation of benzene production and extensive simultaneous reoxidation of Mo, resulting in complete removal of the Mo_2C species and concomitant formation of higher oxidation states including Mo^{6+}, Mo^{5+}, and Mo^{4+}. A similar effect on the formation of benzene and reoxidation of Mo_2C was also observed when an equivalent amount of H_2O was added (10). It may be concluded, therefore, that neither Mo^{6+} ions nor partially reduced Mo ions are active molybdenum species.

Solymosi and co-workers reported poor performance for methane conversion over both unsupported Mo_2C (having a surface area of 1.1 m^2/g) and a physical mixture of 1.4 wt% Mo_2C and ZSM-5 (6). The authors also examined the effect of reoxidation of the 1.4% Mo_2C/ZSM-5 mixture on its behavior for methane conversion and formation of benzene. It was observed that partially (15 to 50%) oxidized Mo_2C/ZSM-5 displayed much better catalytic behavior than that observed for the original Mo_2C/ZSM-5 sample. It was concluded that Mo_2C–MoO_2 with an oxygen deficiency may be the active species for methane activation and formation of ethylene. It should be pointed out that an induction period always occurred for the formation of benzene over these partially oxidized Mo_2C/ZSM-5 samples, and that the amount of oxygen consumed (as CO, CO_2, and H_2O) during the induction period was essentially identical to that used for the oxidation of Mo_2C before reaction. This observation indicates that the formation of benzene reaches a maximum (or steady state) only after virtually all of the Mo oxides are completely reduced, although the conversion of methane reaches a maximum over a partially oxidized Mo_2C/ZSM-5 sample. These results, therefore, are consistent with our postulate that the carbide, Mo_2C, rather than the oxygen-deficient MoO_2 suggested by the above authors, is the active species for methane conversion to benzene. In their most recent studies, however, Solymosi and co-workers (7, 8) also concluded that Mo_2C is the principal species involved in the initial activation of CH_4. The enhanced performance of the Mo_2C/ZSM-5 sample after partial oxidation observed in their earlier studies may have resulted from improved dispersion of Mo during the oxygen pretreatment.

Distribution of Mo in ZSM-5 Zeolite

The phenomenon of spreading and/or dispersion of Mo oxides on various oxide supports, particularly alumina, silica, and zeolites, has been intensively studied recently (37–39). It has been proposed, for example, that Mo species, deposited by conventional wet impregnation using aqueous ammonium heptamolybdate (AHM) solution, are present inside the channels of a Mo/NaY zeolite. However, information concerning the distribution of Mo in ZSM-5 zeolite is scarce and still largely speculative (11, 12, 19, 21). In the present study, the distribution of Mo in the Mo/ZSM-5 catalyst was characterized using XPS, ISS, and FT-IR techniques.

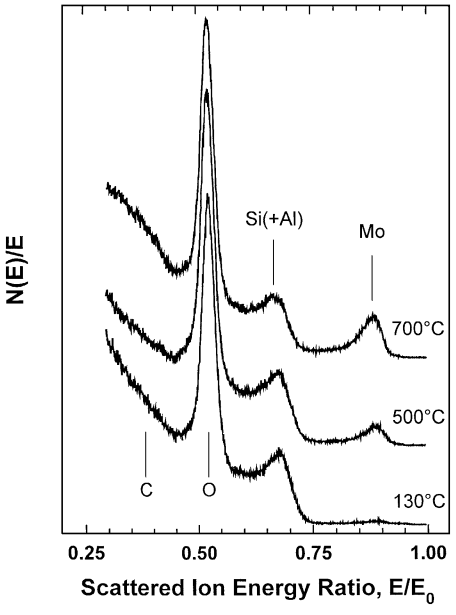

FIG. 6. ISS spectra of 2 wt% Mo/ZSM-5 catalyst calcined at different temperatures.

ISS is a useful method for analyzing the chemical composition of the catalyst surface because of its sensitivity to the outermost atomic layer. Figure 6 shows ISS spectra of the 2% Mo/ZSM-5 catalyst after calcination at different temperatures in O_2. (Similar results were obtained when the sample was heated under a flow of He at the same temperatures). Si and Al are indistinguishable by the ISS technique when using $^3He^+$ ions, particularly when the Si/Al ratio is large, as in the case of ZSM-5. From Fig. 6 it can be observed that C, O, Si(+Al), and Mo are all present on the external surface of the catalyst calcined at the different temperatures. The C peak is not well resolved at the E/E_0 ratio of 0.419 due to its low sensitivity.

Only a very small Mo peak was detected for the sample dried at 130°C for 5 h. Moreover, the intensity of the peak was almost independent of the sputtering time for the sample after heating at this low temperature, although a slight increase in the Mo peak intensity was observed after a long sputtering period, presumably due to redistribution/adsorption of the sputtered Mo species. XPS spectra show that the near-surface concentration of Mo in the 2% Mo/ZSM-5 that was dried at 130°C was only 0.19 at.%. This value is much smaller than 0.42 at.%, which would be the near-surface concentration of the Mo if it were uniformly distributed. In addition, XRD results showed no detectable crystalline phase other than that of the zeolite

support. For a sample having a Mo loading of only 2 wt% in ZSM-5 zeolite, a crystalline Mo-containing phase, if present, would be difficult to detect by XRD if the crystallite sizes were smaller than ca. 50 Å. Since the mean free path of Mo3*d* photoelectrons is 16–17 Å (40), these results suggest that Mo species in the dried sample are present as small (30–50 Å) crystallites of AHM on the external surface of the zeolite. This conclusion is further supported by the fact that the surface concentration of Mo indicated by the ISS spectra did not change after sputtering for 0.5 h with 4 keV Ar^+ ions, which would have exposed more Mo had some been present within the zeolite channels in addition to that on the external surface.

The intensity of the Mo ISS peak increased considerably, relative to that of Si(Al), after calcination in O_2 at 500°C for 4 h (Fig. 6). When the sample was treated in O_2 at 700°C for an additional 0.5 h, the relative intensity of the Mo peak increased even further. Since the 2 wt% Mo loading is equivalent to about two to three monolayers on the ZSM-5 external surface, the intensity of the Si(Al) peak would be expected to decrease to essentially zero if the Mo were completely and uniformly distributed on the ZSM-5 surface. As shown in Fig. 6, however, the relative intensity of the Si(Al) peak did not decrease significantly with increasing treatment temperature, although the intensity of the Mo peak increased markedly after calcination at 500 and, particularly, 700°C, suggesting that the Mo species spread over the surface, but did not become uniformly dispersed on the external surface of the zeolite. It appears that the dispersion of molybdenum oxide species on the surface of ZSM-5 may occur slowly and/or may be restricted to a short distance. Knözinger and co-workers (41) observed that MoO_3 dispersed extensively on Al_2O_3 and TiO_2, but not on SiO_2, after similar thermal treatment.

Additional characterization by ISS and FT-IR indicates that part of the Mo may also diffuse into the zeolite channels during calcination at high temperatures. Figure 7, for example, shows the effect of 4 keV Ar^+ ion sputtering on the ISS spectra of the 2% Mo/ZSM-5 catalyst calcined at 700°C for 0.5 h. (In these experiments, the Ar^+ ion beam was rastered over a 5 × 5-mm area during sputtering to ensure that the He^+ ions collected in the subsequent ISS spectra came only from the area sputtered.) The variation of the Mo/Si peak intensity ratio with sputtering time allows one to obtain information about the distribution of Mo in the channels of the ZSM-5. As the sputtering time increased, the C peak intensity decreased, and the Si(Al) peak correspondingly increased, suggesting that fresh surface was being exposed. The intensity of the Mo peak gradually decreased, but did not vanish, even after sputtering for as long as 2 h. Since no Mo is present in the form of large crystallites on the external surface of the ZSM-5 after calcination at 700°C, as discussed above, it is most likely that the small Mo peak that remains after extensive sputtering is due to Mo species

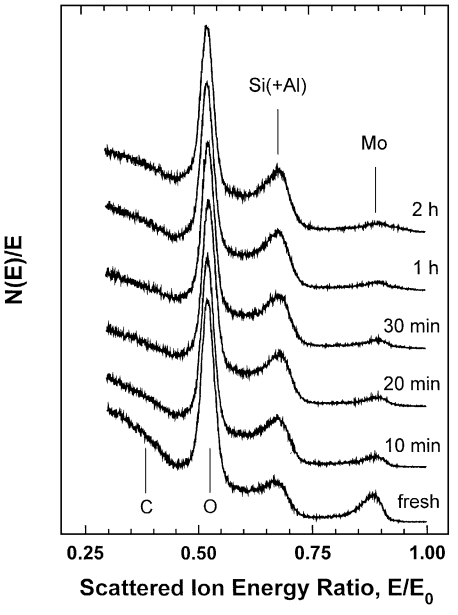

FIG. 7. Effect of Ar^+ sputtering time on ISS spectra of 2 wt% Mo/ZSM-5 calcined at 700°C in O_2 for 0.5 h.

that are inside the channels of the zeolite, rather than from a residue of surface Mo. These results clearly indicate that some Mo does diffuse into the channels of ZSM-5 during calcination at 700°C.

More direct information about the dispersion of Mo on ZSM-5 was obtained from FT-IR experiments in which the effects of Mo impregnation on the O–H stretching modes of the zeolite were examined. Figure 8 shows IR spectra of the pure H-ZSM-5 starting material and of 2% Mo/ZSM-5 in the region of the zeolitic O–H stretching modes, after thermal treatment in flowing He at 700°C for the indicated times. All of the spectra were recorded after quenching the treated sample in He to room temperature.

As shown in Fig. 8a, pure H-ZSM-5 contains three principal types of hydroxyl groups. One of these, having a vibrational frequency of 3611 cm^{-1}, is associated with the Brønsted acidity of the zeolite (42–44). The intensity of this band correlates with the aluminum content of the zeolite (43) and with the extent of proton exchange (44). A second hydroxyl group, having a stretching frequency at 3747 cm^{-1}, has been attributed to silanol groups that terminate the zeolite lattice. i.e., those on the external surface (42, 43). The weak band at about 3670 cm^{-1} has been attributed to hydroxyl groups that are associated with extra framework aluminum species (45). A separate ^{27}Al NMR experiment confirmed the presence of a significant amount of extra framework aluminum in this H-ZSM-5 zeolite.

It is apparent that all three types of OH groups in H-ZSM-5 are thermally stable during treatment in flowing He at 700°C. The intensities of the various OH bands

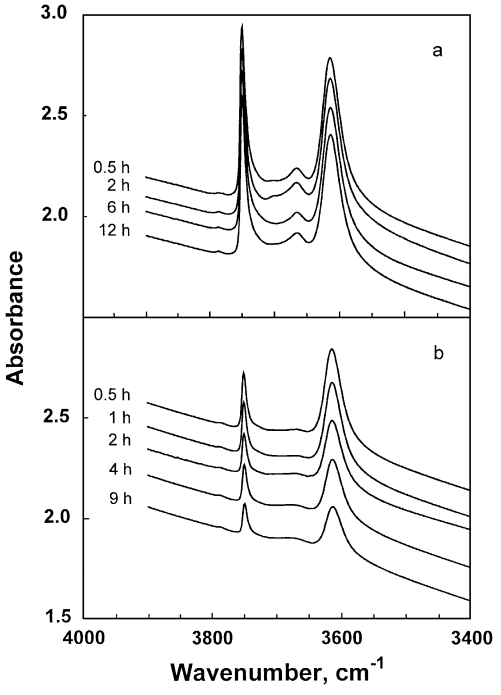

FIG. 8. Infrared spectra of: (a) pure H-ZSM-5 and (b) 2 wt% Mo/ZSM-5 catalyst treated for various times at 700°C in He.

were virtually unchanged, even after treatment at this temperature for 12 h. It should be mentioned that the overall intensities of the various hydroxyl bands reached a maximum after treatment in flowing He at 500 to 600°C and did not decrease significantly following treatment at 700°C. Dehydroxylation of the Brønsted OH groups at 3611 cm^{-1} becomes significant only after heating at 900°C; even at this temperature, however, hydroxyl removal is not complete after heating the sample for 9 h. Dehydroxylation of the terminal surface silanol groups does not occur appreciably, even after heating the sample at 900°C for many hours.

Infrared spectra obtained after heating the 2% Mo/ZSM-5 sample in flowing He at 700°C for various times, are shown in Fig. 8b. Comparison of these spectra with those in Fig. 8a obtained after comparable treatment times reveals that, although the amounts of all three types of OH groups decreased following Mo impregnation, the relative extent of the decrease differed markedly for the various OH species. The weak band at 3670 cm^{-1}, for example, due to OH groups on extra framework aluminum, disappeared almost completely upon Mo impregnation. Similarly, the concentration of OH groups associated with terminal silanol species (3747 cm^{-1}) decreased to a significantly greater extent than did that of the Brønsted acidic OH groups (3611 cm^{-1}) located inside the zeolite channels. Quantitative analysis of the spectra obtained after a 0.5-h treatment at 700°C indicates that impregnation with 2 wt% Mo caused the intensity of the silanol OH band to decrease to ~30% of that observed for the pure HZSM-5, while the Brønsted hydroxyl groups, by contrast, retained ~70% of the intensity observed for the unimpregnated HZSM-5. It should be noted that the intensity of the Brønsted hydroxyl band did not decrease at all when the 2% Mo/ZSM-5 was heated at only 400°C for 1 h, while the silanol groups lost ~50% of their intensity following treatment at this temperature. These observations indicate that impregnated Mo remains primarily on the external surface of the zeolite at treatment temperatures of ≤400°C, and that some of the Mo diffuses into the channels of the zeolite after calcination at 700°C for 0.5 h. These results also suggest that the ISS signal observed for Mo in Fig. 7 after Ar^+ sputtering is primarily due to Mo within the channels of the zeolite.

As shown in Fig. 8b, as the time of calcination was increased, the Mo species continued spreading on the external surface, while simultaneously diffusing into the channels of the ZSM-5. After 9 h of treatment at 700°C, for example, the intensities of both the silanol and the Brønsted hydroxyl bands decreased an additional 50% from the amounts present after only 0.5 h of treatment at this temperature. Moreover, the rates of spreading and/or diffusion of the Mo^{6+} species of the oxide depend strongly on the calcination atmosphere. The spectrum of the hydroxyl groups in a 2% Mo/ZSM-5 sample after calcination in air at only 500°C for 4 h is similar to that obtained for a sample calcined at 700°C in dry O_2 or in He for the same length of time, suggesting that moisture in the air significantly promotes the diffusion process. A similar effect of moisture on the dispersion of Mo has been reported previously to occur for Mo/Al_2O_3, but not for Mo/SiO_2 (41). It should be noted that under CH_4 reaction conditions, most of the molybdenum oxide has already been converted into Mo_2C, and, as a result, the diffusion process is terminated. We have observed, for example, that the band intensities of both principal types of hydroxyl groups on the Mo/ZSM-5 catalyst following initial calcination at 700°C remain essentially unchanged after subsequent exposure to a CH_4/H_2 gas mixture at 700°C.

The decrease in intensities of the three types of O–H stretching bands at 3747, 3611, and 3670 cm^{-1} indicates that the impregnated Mo species are evidently located in the vicinity of these hydroxyl groups. Thus, the terminal zeolitic silanol groups, although essentially nonacidic, may act like Al–OH species on the surface of Al_2O_3, which have been proposed to react with $Mo_7O_{24}^{6-}$ anionic species during the preparation of Mo/Al_2O_3 catalysts (46, 47). It appears, therefore, that silanol groups on H-ZSM-5 are replaced by Mo species on the external surface of the zeolite, since a broadening and/or red-shift of the silanol band at 3747 cm^{-1}, but not an overall decrease in intensity, would be expected if only a strong interaction and not a replacement occurred between the Mo species and the silanol groups. In addition, the ISS results in Fig. 6 confirm that a small part

of the Si was covered with Mo. Similarly, Mo species inside the channels of ZSM-5 may react with the Al^{3+} (both lattice and extra framework), and an extraction of Al cations from the zeolite framework could occur (48, 49), in addition to an exchange with H^+ ions (11).

Based solely on the observed intensity changes of the ν(OH) IR bands, no definitive conclusion can be drawn about the distribution of molybdenum in the ZSM-5 zeolite because the extinction coefficients of the different types of hydroxyl groups are not known. However, a combination of FT-IR and XPS/ISS measurements may allow such information to be obtained. As shown in Figs. 7 and 8, Mo is highly enriched on the external surface of the zeolite, although the absolute amount of Mo within the channels is not known. It would be expected that more Mo may diffuse into the channels of the zeolite when the Mo loading is higher, especially for a Mo/ZSM-5 sample calcined at high temperatures, e.g., $\geq$700°C, for many hours. As a result, the number of acid sites would decrease significantly. We have previously shown (9, 10) that ethylene, the primary product formed from CH_4 reactant on the surface of coke-modified Mo_2C, is converted into benzene and other aromatics on such acid sites within the channels of the ZSM-5 zeolite. The presence of a certain concentration of acid sites in Mo/ZSM-5 catalysts is thus necessary to achieve a high benzene selectivity and a high methane conversion, since the formation of aromatics is thermodynamically favored (10). It is not surprising, therefore, that a Mo/ZSM-5 catalyst with a high Mo loading, e.g., $\geq$5 wt%, displayed both a low methane conversion and poor benzene selectivity (12, 14), except when the catalyst was calcined at a lower temperature (14).

CONCLUSIONS

The distribution and the chemical states of Mo in a 2 wt% Mo/ZSM-5, before and after calcination at different temperatures, were investigated using XPS, ISS, and FT-IR techniques, and correlated with kinetic results for the conversion of methane to benzene. Impregnated molybdenum in the calcined catalyst is initially present as MoO_3, primarily in the form of small crystallites on the external surface of the ZSM-5 zeolite. After treatment at $\leq$400°C, relatively little Mo is present in the channels of ZSM-5, and the acidity of the zeolite is not modified. After calcination at 500°C in O_2, the Mo becomes highly dispersed on the external surface of the zeolite, and part of it diffuses into the channels, causing a decrease in acidity. The Mo distribution, however, is not uniform on the external surface of the zeolite. Although calcination of the catalyst at 700°C for 0.5 h results in improved dispersion of Mo over the external surface and, possibly, inside the channels of the zeolite, uniform monolayer coverage of Mo on the external surface does not occur. The concentration of Mo within the channels of the zeolite increases as the temperature and time of calcination increases. The presence of moisture during the calcination may significantly promote diffusion of Mo into the channels, especially at higher temperatures.

Exposure of a 2 wt% Mo/ZSM-5 catalyst to CH_4 or to CH_4/H_2 at 700°C causes reduction of Mo ions to Mo_2C, rather than to metallic Mo. About 60 to 80% of Mo species are present in the form of Mo_2C after the reaction reaches steady state, but part of the Mo (20–30%) remains present as Mo^{4+} and Mo^{5+} and is not reduced even when the catalyst is treated in CH_4 or CH_4/H_2 at 700°C for many hours. The formation of Mo_2C corresponds well with the time of the initial activation period for the production of benzene, indicating that carbidic molybdenum species are the active centers for the activation of methane. This assumption is supported by the inhibiting effect of CO_2 or moisture on the formation of benzene (10). Since preformation of Mo_2C on the catalyst, without coke deposition, does not completely eliminate the induction period, it is believed that the clean surface of Mo_2C may be too reactive to form higher hydrocarbons and, thus, that a coke-modified Mo_2C surface may be the actual active species in the formation of ethylene as the reaction intermediate.

ACKNOWLEDGMENT

The authors gratefully acknowledge financial support of this research by the National Science Foundation, under Grant CHE-9520806.

REFERENCES

1. Bragin, O. V., Vasina, T. V., Preobrazhenskii, A. V., and Minachev, Kh. M., *Izv. Akad. Nauk SSSR, Ser. Khim.* **3**, 750 (1989); Vasina, T. V., Preobrazhenskii, A. V., Isaev, S. A., Chetina, O. V., Masloboishikova, O. V., and Bragin, O. V., *Kinet. Catal.* **35**, 93 (1994).
2. Belgued, M., Pareja, P., Amariglio, A., and Amariglio, H., *Nature* **352**, 789 (1991); Belgued, M., Amariglio, A., Pareja, P., and Amariglio, H., *J. Catal.* **159**, 441, 449 (1996).
3. Koerts, T., Deelen, M. J. A. G., and van Santen, R. A., *J. Catal.* **138**, 101 (1992).
4. Wang, L., Tao, L., Xie, M., Huang, J., and Xu, Y., *Catal. Lett.* **21**, 35 (1993).
5. Solymosi, F., Erdohelyi, E., and Szoke, A., *Catal. Lett.* **32**, 43 (1995).
6. Solymosi, F., Szoke, A., and Cserenyi, J., *Catal. Lett.* **39**, 157 (1996).
7. Szöke, A., and Solymosi, F., *Appl. Catal.* **142**, 361 (1996).
8. Solymosi, F., Cserényi, J., Szöke, A., Bánsági, T., and Oszkó, A., *J. Catal.* **165**, 150 (1997).
9. Wang, D., Lunsford, J. H., and Rosynek, M., "14th North American Meeting of the Catalysis Society Preprints," Snowbird, UT, 1995.
10. Wang, D., Rosynek, M., and Lunsford, J. H., *Topics Catal.* **3**, 289 (1996).
11. Xu, Y., Liu, S., Wang, L., Xie, M., and Guo, X., *Catal. Lett.* **30**, 135 (1995).
12. Chen, L., Lin, L., Xu, Z., Li, X., and Zhang, T., *J. Catal.* **157**, 190 (1995).
13. Wang, L., Xu, Y., Xie, M., Liu, S., and Tao, L., *Stud. Surf. Sci. Catal.* **94**, 495 (1995).
14. Xu, Y., Shu, Y., Liu, S., Huang, J., and Guo, X., *Catal. Lett.* **35**, 233 (1995).
15. Wong, S., Xu, Y., Wang, L., Liu, S., Li, G., Xie, M., and Guo, X., *Catal. Lett.* **38**, 39 (1996).

16. Xu, Y., Liu, W., Wong, S., Wang, L., and Guo, X., *Catal. Lett.* **40**, 207 (1996).
17. Chen, L., Lin, L., Xu, Z., Zhang, T., and Li, X., *Catal. Lett.* **39**, 169 (1996).
18. Nefedov, V. I., Firsov, M. N., and Shaplygin, I. S., *J. Electron Spectrosc. Relat. Phenom.* **26**, 65 (1982).
19. Valyon, J., and Meszaros-Kis, A., *in* "Zeolites: Facts, Figures, Future" (P. A. Jacobs and R. A. van Santen, Eds.), Vol. 49, p. 1015. Elsevier, Amsterdam, 1989.
20. Cid, R., Llambias, F. J. G., Fierro, J. L. G., Agudo, A. L., and Villasenor, J., *J. Catal.* **89**, 478 (1984).
21. Agudo, A. L., Benitez, A., Fierro, J. L. G., and Palacios, J. M., *J. Chem. Soc., Faraday Trans. I* **88**(3), 385 (1992).
22. Ledoux, M. J., Huu, C. P., Guille, J., and Dunlop, H., *J. Catal.* **134**, 383 (1992).
23. Wagner, C. D., and Taylor, J. A., *J. Electron Spectrosc. Relat. Phenom.* **20**, 83 (1980).
24. Brainard, W. A., and Wheeler, D. R., *J. Vacuum Sci. Technol.* **15**, 1801 (1978).
25. Lee, J. S., Volpe, L., Ribeiro, F. H., and Boudart, M., *J. Catal.* **112**, 44 (1988).
26. Lee, J. S., Oyama, S. T., and Boudart, M., *J. Catal.* **106**, 125 (1988).
27. Pearlstine, K. A., and Friend, C. M., *J. Am. Chem. Soc.* **107**, 5898 (1985).
28. Kelly, D. G., Salmeron, M., and Somorjai, G. A., *Surf. Sci.* **175**, 465 (1986).
29. Wang, L., and Tysoe, W. T., *J. Catal.* **128**, 320 (1991).
30. Chen, J. G., *J. Catal.* **154**, 80 (1995).
31. DeVries, J. E., Yao, H. C., Bird, and Gandhi, H. S., *J. Catal.* **84**, 8 (1983).
32. Briggs, D., and Seah, M. P., "Practical Surface Analysis," 2nd ed., Vol. 1. Wiley, New York, 1990.
33. Ramqvist, L., Hamrin, K., Johansson, G., Fahlman, A., and Nordling, C., *J. Phys. Chem. Solids* **30**, 1835 (1969).
34. Grünert, W., Stakheev, A. Y., Mörke, W., Feldhaus, R., Anders, K., Shpiro, E. S., and Minachev, K. M., *J. Catal.* **135**, 269 (1992).
35. Wang, J., Castonguay, M., McBreen, P. H., Ramanathan, S., and Oyama, S. T., *in* "The Chemistry of Transition Metal Carbides and Nitrides" (S. T. Oyama, Ed.), p. 426. Blackie, London, 1996.
36. Dai, P. E., and Lunsford, J. H., *J. Catal.* **64**, 173 (1980); Yang, T., and Lunsford, J. H., *J. Catal.* **103**, 55 (1987).
37. Knözinger, H., and Taglauer, E., *in* "Catalysis" (J. J. Spivey, Ed.), Vol. 10, p. 1. Royal Chem. Soc., Cambridge, 1993; and references therein.
38. Banares, M. A., Hu, H., and Wachs, I. E., *J. Catal.* **150**, 407 (1994).
39. Zhang, W., Desikan, A., and Oyama, S. T., *J. Phys. Chem.* **99**, 14468 (1995).
40. Tanuma, S., Powell, C. J., and Penn, D. R., *Surf. Interface Anal.* **11**, 577 (1988); Tanuma, S., Powell, C. J., and Penn, D. R., *Surf. Interface Anal.* **20**, 77 (1993).
41. Leyrer, J., Margraf, R., Taglanuer, E., and Knözinger, K., *Surf. Sci.* **201**, 603 (1988); Margraf, R., Leyrer, J., Knozinger, K., and Taglanuer, E., *Surf. Sci.* **189/190**, 842 (1987).
42. Vedrine, J. C., Auroux, A., Bolis, V., Dejaifve, P., Naccache, C., Wierzchowski, P., Derouane, E. G., Nagy, J. B., Gilson, J., van Hooff, J., van den Berg, J. P., and Wolthuizen, J., *J. Catal.* **59**, 248 (1979).
43. Topsøe, N., Pedersen, K., and Derouane, E. G., *J. Catal.* **70**, 41 (1981).
44. Jacobs, P. A., and von Ballmoos, R., *J. Phys. Chem.* **86**, 3050 (1982).
45. Campbell, S. M., Bibby, D. M., Coddington, J. M., Howe, R. F., and Meinhold, R. H., *J. Catal.* **161**, 338 (1996).
46. Arnoldy, P., van den Heijkant, J. A. M., de Bok, G. D., and Moulijn, J. A., *J. Catal.* **92**, 35 (1985).
47. Massoth, F. E., *Adv. Catal.* **27**, 265 (1979).
48. Ezzamarty, A., Catherine, E., Cornet, D., and Hemidy, J. F., *in* "Zeolites: Facts, Figures, Future" (P. A. Jacobs and R. A. van Santen, Eds.), Vol. 49, p. 1025. Elsevier, Amsterdam, 1989.
49. Sanz, J., Fornes, V., and Corma, A., *J. Chem. Soc., Faraday Trans. I* **84**, 3113 (1988).